Metabolism modelling in rivers with unsteady flow conditions and transient storage zones

Devanshi Pathak[1,2], Benoît O L Demars[3]

[1]UK Centre for Ecology and Hydrology, Wallingford, United Kingdom
[2]School of Geography and water@leeds, University of Leeds, Leeds, United Kingdom
[3]Norwegian Institute for Water Research, Gaustadalleen 21, 0349 Oslo, Norway

Key Points:

- A metabolism model is developed by coupling an unsteady flow routing model with the two-station stream metabolism model.
- The influence of transient storage and flow regulation at upstream and downstream ends on solute transport time is considered in the model.
- The model successfully estimates metabolism in the case study, but requires accurate characterisation of solute travel time parameters.

Corresponding author: Devanshi Pathak, devpat@ceh.ac.uk

Abstract

Whole-stream metabolism models are generally implemented with a steady flow assumption that does not hold true for many systems with sub-daily flow variation, such as river sections downstream of dams. The steady flow assumption has confined metabolism estimation to a limited range of river environments, thus limiting our understanding about the influence of hydrology on biological production in rivers. Therefore, we couple a flow routing model with the two-station stream metabolism model to estimate metabolism under unsteady flow conditions in rivers. The model's applicability is further extended by including advection-dispersion processes to facilitate metabolism estimation in transient storage zones. Metabolism is estimated using two approaches: (1) an accounting approach similar to the conventional two-station method and (2) an inverse approach that estimates metabolism parameters using least-squares minimisation method. Both approaches are complementary since we use outputs of the accounting approach to constrain the inverse model parameters. The model application is demonstrated using a case study of an 11 km long stretch downstream of a hydropower plant in the River Otra in southern Norway. We present and test different formulations of the model to show that users can make an appropriate selection that best represents hydrology and solute transport mechanism in the river system of interest. The inclusion of unsteady flows and transient storage zones in the model unlocks new possibilities for studying metabolism controls in altered river ecosystems.

Plain Language Summary

Whole-stream metabolism is not only an integrative measure of river ecosystem health, but also characterises carbon transformations in freshwater systems. Therefore, it is important to accurately estimate whole-stream metabolism in diverse river environments. To achieve this, we focus on addressing two limitations in the current metabolism models. Firstly, we include the influence of sub-daily flow variation on metabolism. Such a variation is common below hydropower dams and has a potential to negatively impact metabolism downstream of dams. Secondly, we include the influence of transient storage zones on metabolism. These storage zones are like dead zones in rivers, where the movement of water and solutes may be slowed down compared to the rest of the flowing river. These zones may significantly influence metabolism because the travel time of water and solute particles in these zones is higher. Using a case study of the River Otra

in southern Norway, we show that the model successfully includes the influence of aforementioned river environments in whole-stream metabolism estimation. The model provides opportunities to estimate metabolism in a wider range of river environments, which in turn will help reduce uncertainties in our global estimates of freshwater carbon fluxes.

1 Introduction

Biotic CO_2 emissions from rivers can be estimated through the metabolic balance of rivers, thus contributing to our understanding of the global carbon cycle (Demars et al., 2016; Hotchkiss et al., 2015; Raymond et al., 2013). Whole-stream metabolism characterises carbon fixation and mineralisation through gross primary production (GPP) and ecosystem respiration (ER) in streams and rivers. GPP and ER are integral measures of riverine biological processes (Bernhardt et al., 2018) and can serve as important indicators of whole-river health (Ferreira et al., 2020; Von Schiller et al., 2017; Young et al., 2008).

Ecologists have developed robust models for whole-stream metabolism estimation based on diel oxygen changes in open channels (Demars et al., 2015; Holtgrieve et al., 2016; Odum, 1956) including book-keeping methods with Monte-Carlo simulation (Demars, 2019) and inverse models with Bayesian procedure (Appling, Hall Jr, et al., 2018; Hall et al., 2016; Holtgrieve et al., 2010). However, these models were developed for reach-scale estimation and for a limited range of river environments (Appling, Read, et al., 2018). For example, the open-channel metabolism models do not account for the influence of sub-daily flow variation and transient storage zones on dissolved oxygen variation at river-network scale despite these features being prevalent in many rivers due to flow regulation (Zimmerman et al., 2010) and channel hydromorphological characteristics (Kurz et al., 2017), respectively. Civil engineers have also produced water quality models for oxygen prediction to address river sanitation issues (Beck & Young, 1975; Streeter & Phelps, 1925). These models are applicable to entire river networks (Cox, 2003a, 2003b), whereas this is just emerging in the ecological literature (Pathak et al., 2022; Segatto et al., 2020, 2021). Therefore, we can integrate implementations from both these fields to build parsimonious models applicable at river-network scale and to a wider range of river environments than those currently studied through open-channel metabolism models.

Quantification of transient storage in metabolism models may be crucial as these zones are potential hotspots of metabolism in rivers due to longer residence times (Argerich et al., 2011; Fellows et al., 2001; Mulholland et al., 2001). Transient storage zones are characterised by stagnant pockets of water due to presence of biofilms, dense patches of aquatic plants, hyporheos or eddies of deep pools (Bencala & Walters, 1983; Bottacin-Busolin et al., 2009; Ensign & Doyle, 2005). Several models have been developed to simulate the impact of transient storage on solute transport in rivers such as the Transient Storage Model (Bencala & Walters, 1983; Manson et al., 2001; Runkel, 1998) and the Aggregated Dead Zone (ADZ) model (Beer & Young, 1983; Wallis et al., 1989). The proportion of transient storage and the exchange rate of water molecules between the main channel and the storage zone may change with flow (Manson et al., 2010; Wallis & Manson, 2018), but current models were designed to work under steady flows.

The assumption of steady flow conditions in metabolism models may not be valid in regulated rivers. Wide-spread flow regulation for reservoir operations in rivers around the world has altered the frequency and magnitude of sub-daily flow variation and consequently impacted healthy ecosystem functioning (Poff & Zimmerman, 2010). The timings and magnitude of flow releases determine trends in metabolism. Reduction in flow variability can elevate downstream metabolism (Aristi et al., 2014), whereas abrupt high flow releases can reduce tailwater metabolism (Uehlinger et al., 2003). The studies analysing flow regulation impacts on ecosystem metabolism have mainly looked at coarser temporal scale using Odum (1956)'s two-station method at a river-reach scale, where homogeneous hydraulic conditions are assumed over a period of day, i.e. impact of average daily flow on average daily metabolism (e.g. Aristi et al., 2014; Chowanski et al., 2020; Uehlinger et al., 2003). However, metabolism models need to account for sub-daily flow variability, especially considering recent trends in the rapidly changing energy markets (e.g. switch to renewable energy) that may enhance the sub-daily variability in flow (hydropeaking) in tailwaters (Ashraf et al., 2018). To address these limitations, a river network model for stream metabolism requires the run of a flow routing model ahead of implementing the two-station method (Cimorelli et al., 2016; Payn et al., 2017; Whitehead et al., 1997). The prospect of simply adding water transient storage using advection-dispersion equations (Chapra & Runkel, 1999; Demars et al., 2015) to these more complicated models is daunting because many additional parameters would need to be estimated or well con-

strained to apply the models at river-network scale under varying flow conditions, as exemplified with nutrient cycling (Ye et al., 2012).

This study overcomes these limitations through development of a parsimonious model for Metabolism estimation in rivers with Unsteady Flow conditions and Transient storage zones (MUFT) that can be extended to a river-network scale. To demonstrate the model's development and implementation, we used a case study of the River Otra in southern Norway. The MUFT model was implemented along an 11 km river stretch downstream of a hydropower plant, where dam operations cause significant diel fluctuations in flow. To include the influence of diel flow variation in the MUFT model, we coupled a simple unsteady flow routing model adapted from the QUASAR (QUAlity Simulation Along River systems) model (Whitehead et al., 1997) with a two-station stream metabolism model (Odum, 1956). The study stretch also demonstrates delayed oxygen transport compared to water velocity, which could be attributed either to the transient storage created from excessive plant growth in the river reach or to the dual flow regulation by dams at the upstream and downstream ends of the study stretch. To account for these probable mechanisms of oxygen transport, we tested two model formulations, (1) ADZ model that accounts for transient storage zones (Wallis et al., 1989) and (2) ADV (advection) model that accounts for dual flow regulation impact on oxygen transport (Beck & Young, 1975). In the MUFT model, these formulations (ADV or ADZ) are coupled with the unsteady flow routing and the two-station stream metabolism models. Previously, studies have proposed modifications in the QUASAR flow routing model to simulate unsteady flows (Sincock & Lees, 2002) as well as proposed coupling of ADZ and original QUASAR (steady flow) models to simulate non-conservative solutes (Lees et al., 1998). The MUFT model combines these efforts by coupling the unsteady QUASAR model and the ADZ model to simulate non-conservative solutes.

In this study, we show metabolism estimation using both inverse and accounting (book-keeping) approaches in the MUFT model. While the accounting method is not predictive, it allows an independent estimation of the light parameters for GPP that are used to better constrain the inverse model and avoid issues of equifinality. The modelling approaches presented in this study not only provide theoretical benefits for studying the impact of transient storage zones and unsteady flows on metabolism dynamics, but also promote practical applications for the management of tailwater river ecosystems.

2 Theory

We first selected a flow routing model to simulate discharge downstream of a hydropower plant, with upstream flow boundary conditions (from e.g. gauging station, rainfall-runoff simulations) as model input. We present the flow model equations in this section, but any flow routing model of user's preference can be used. Further, we present associated metabolic models of dissolved oxygen (DO) concentrations under unsteady flow conditions with increasing complexity. In the next section, we show how to apply these models to a case study.

2.1 Flow routing model

To simulate unsteady flows in the MUFT approach, we adapted the flow routing model proposed by Sincock and Lees (2002), who based their approach on the QUASAR model (Whitehead et al., 1997) originally designed for slowly time-varying flows (quasi steady-state). Because of the steady flow assumption, the original QUASAR model assumes the flow and solute travel times to be equal. However, under unsteady flow conditions, the travel time of flood wave can be expressed in terms of kinematic wave velocity (celerity), which is higher than the mean flow velocity (Sincock et al., 2003) and consequently, solute velocity. The ratio m of the average celerity (c, m s^{-1}) to the average flow velocity (u, m s^{-1}) is expressed following Sincock et al. (2003),

$$m = \frac{c}{u} = \frac{dQ/dA}{Q/A} \tag{1}$$

where Q is discharge (m^3 s^{-1}), A is the cross section area of flow and m may be approximated as 5/3 (Chapra, 2008).

The celerity (c, m s^{-1}) of the flood wave for a reach of length L (m) is,

$$c = \frac{L}{T_{flow}} \tag{2}$$

where T_{flow} represents the travel time of the flood wave (s).

It is assumed that T_{flow} may be partitioned into dispersion (T_{fladz}) and advection (τ_{fl}) terms using a fraction of retention F_r,

$$T_{fladz} = F_r \times T_{flow} \tag{3}$$

$$\tau_{fl} = (1 - F_r) \times T_{flow} \tag{4}$$

The flow routing model includes a simple mass-balance of incoming and outgoing flows and assumes fixed channel width with rectangular cross-section. Lateral groundwater inflows and discharge from small tributaries were assumed to be negligible within reaches. In a river network, the flow of major tributaries may be inserted at the upstream edge of a reach. River reaches may be represented as a series of non-linear reservoirs. The flow model simulates water transport through a series of n non-linear reservoirs followed by a time lag parameter (τ_{fl}, s) that lags the routed hydrograph without attenuation (Figure 1a). The changes in flow are represented as,

$$\frac{dQ_t}{dt} = \frac{Q_{i,t-\tau_{fl}} - Q_t}{F_r T_{flow}} \tag{5}$$

where Q is the flow leaving the reach at time t, Q_i is the flow coming into the reach at time t. Eq. 5 accounts for the travel time (T_{flow}) derived from celerity (Eq. 2) as opposed to the travel time derived from mean flow velocity as is commonly done in original QUASAR model applications.

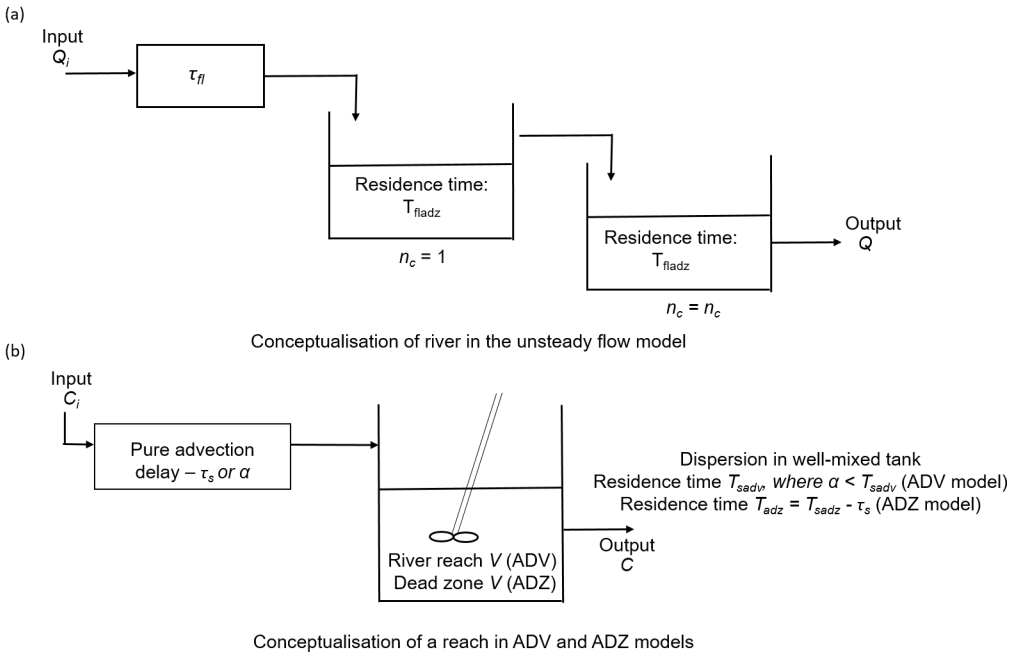

Figure 1. Conceptualisation of river reaches in the (a) unsteady flow model adapted from Sincock and Lees (2002) and (b) ADZ model adapted from Lees et al. (2000) for conservative solute C

2.2 Metabolic model in a well-mixed reach under unsteady flow conditions

We developed the metabolic model of DO dynamics (Eq. 6) by combining two approaches, (1) the conservative solute transport model proposed by Whitehead et al. (1997) to simulate DO transport with unsteady flows and (2) the two-station stream metabolism method proposed by Odum (1956) to simulate in-stream DO sources and sinks from metabolism and air-water gas exchange processes. The detailed proofs of both models were given in the original publications. Note that Eq. 6 does not account for water transient storage.

$$\frac{dC_t}{dt} = \frac{Q_{i,t}}{(Q_t \times T_u)}(C_{i,t} - C_t) + \frac{1}{z_t}(P_{GPP,t} - R_{ER,t}) + k(C_{s,t} - C_t) \quad (6)$$

where C_i is the incoming DO in the reach (mg O_2 L^{-1} equivalent to g O_2 m^{-3}), C is the DO leaving the reach (mg O_2 L^{-1}), P_{GPP} is the gross primary production (g O_2 m^{-2} min^{-1}), R_{ER} is the ecosystem respiration (g O_2 m^{-2} min^{-1}), k is the gas exchange coefficient (min^{-1}) and C_s is the expected oxygen solubility (mg O_2 L^{-1}). T_u (min) represents the mean flow travel time, which is equal to the solute travel time for a well-mixed reach.

2.3 Metabolic model with pure advection and a well-mixed reach under unsteady flows (ADV model)

In long reaches where solute transport is dominated by advective transport as opposed to dispersion, it may be necessary to explicitly take into account pure advection as shown in Eq. 7 (Beck & Young, 1975; Odum, 1956). The ADV formulation accounts for the effect of dual water regulation by dams at upstream and downstream ends of the study reach. The dual water regulation results in apparent faster water velocity compared to the solute velocity due to the early release of water by the downstream dam before the water from the upstream dam reaches the downstream dam.

$$\frac{dC_t}{dt} = \frac{Q_{i,t-\alpha}}{(Q_t \times T_{sadv})}(C_{i,t-\alpha} - C_t) + \frac{1}{z_t}(P_{GPP,t} - R_{ER,t}) + k(C_{s,t} - C_t) \quad (7)$$

$$\alpha = F_{adv} \times T_{sadv} \quad (8)$$

where F_{adv} is the advection delay coefficient. The addition of pure advection α (see Table 1) in the first term of the equation allows to have the two DO concentration curves in phase without modifying their shape (simple time translation), with $\alpha \leq T_{sadv}$ (Beck & Young, 1975). Note that T_{sadv} is equivalent to T_u for the ADV model.

2.4 Metabolic model with pure advection and transient storage (dispersion) under unsteady flows (ADZ model)

The influence of transient storage in the metabolic model is included using the ADZ concept (Beer & Young, 1983; Wallis et al., 1989) as proposed by Sincock and Lees (2002), who coupled the unsteady QUASAR flow model with the ADZ model for a conservative solute. ADZ model was selected for its simplicity and its conceptual similarity to the unsteady QUASAR flow model (Figure 1). The original QUASAR model assumes the river reach to be a perfectly mixed system. ADZ model conceptualises the river reach as an imperfectly mixed system, where solute is subjected to pure advection followed by dispersion in a lumped active mixing zone (Beer & Young, 1983; Lees et al., 2000; Wallis et al., 1989). The metabolic model becomes:

$$\frac{dC_t}{dt} = \frac{Q_{i,t-\tau_s}}{(Q_t \times T_{adz})}(C_{i,t-\tau_s} - C_t) + \frac{1}{z_t}(P_{GPP,t} - R_{ER,t}) + k(C_{s,t} - C_t) \tag{9}$$

The ADZ model partitions the overall solute travel time T_{sadz} into dead-zone residence time T_{adz} and advection lag τ_s, equivalent to partitioning total reach volume into the volume of water transient storage and main channel.

$$T_{adz} = T_{sadz} - \tau_s \tag{10}$$

For reaches affected by transient storage, the effective solute transport velocity (u_s) is lower than the mean flow velocity (u) due to solute retention in the storage zone. The relationship between these velocities can be described using a solute-lag coefficient β (Lees & Camacho, 2000) as,

$$u_s = \frac{u}{1+\beta} \tag{11}$$

Considering Eq. 1, Eq. 2 and Eq. 11, travel time and advection lag for a solute in the ADZ model can be described in terms of flow parameters (Sincock, 2002),

$$T_{sadz} = m(1+\beta)T_{flow} \tag{12}$$

$$\tau_s = m(1+\beta)\tau_{fl} \tag{13}$$

2.5 Modified two-station model for the accounting method

Eq. 9 can be simplified to derive net ecosystem production ($P_{NEP} = P_{GPP} - R_{ER}$) using Euler finite-difference approach, which gives the two-station accounting approach

under varying discharge,

$$P_{NEP,t} = \left(\frac{C_{t+\Delta t} - C_t}{\Delta t} - \frac{Q_{i,t-\tau_s}}{(Q_t \times T_{adz})} (C_{i,t-\tau_s} - C_t) - k(C_{s,t} - C_t) \right) z_t \tag{14}$$

Note that Eq. 14 can easily be adjusted for the other metabolic models presented above (Eq. 6 and Eq. 7). This approach allows to estimate average R_{ER} during the dark hours (photosynthetically-active radiation (PAR) < 1 µmol-photons m^{-2} s^{-1}) and deduce $P_{GPP,t}$ by difference ($P_{NEP,t} - R_{ER,t}$) during the light hours assuming constant R_{ER} throughout the day (see Demars et al., 2015). Daily GPP (P_{GPP}) is simply the sum of $P_{GPP,t}$ throughout a day,

$$P_{GPP} = \frac{\int_{t_0}^{t_{end}} P_{GPP,t}\, dt}{1\, day} \tag{15}$$

2.6 Photosynthesis-light relationship

The accounting method has the advantage, over the inverse modelling approach, of deriving instantaneous and daily GPP without making any assumption on the photosynthesis-light relationship. The most appropriate link function may thus be selected by plotting $P_{GPP,t}$ as a function of PAR_t. The function is substituted to $P_{GPP,t}$ in the metabolic models (Eq. 6, Eq. 7 or Eq. 9). The parameters of the link function may be used as constants or enabled to constrain the priors (through their uncertainties) in the inverse model, thus reducing issues of equifinality. Here, instantaneous gross primary production (P_{GPP}) was modelled as a function of PAR with a Michaelis-Menten type equation to include the light-saturation effect on photosynthesis (Demars et al., 2011),

$$P_{GPP,t} = \frac{P_{GPPmax} \times E_{PAR,t}}{k_{PAR} + E_{PAR,t}} \tag{16}$$

where $E_{PAR,t}$ is the photosynthetically-active radiation (µmol-photons m^{-2} s^{-1}) at time t, P_{GPPmax} is the maximum GPP (g O_2 m^{-2} min^{-1}) and k_{PAR} is the PAR at which half the P_{GPPmax} is attained (µmol-photons m^{-2} s^{-1}).

P_{GPPmax} and k_{PAR} in the inverse model were estimated using a least-squares minimisation algorithm. It is implicitly assumed that light conditions are spatially uniform along the modelled channel length and PAR only varies with time.

2.7 Dissolved oxygen saturated concentration

The expected oxygen solubility (C_s, mg L^{-1}) was estimated from Standing Committee of Analysts (1989) as follows,

$$C_s = \frac{C_{atm}(P - V_P)}{101.325 - V_P} \tag{17}$$

where C_{atm} is the oxygen solubility under normal atmospheric pressure (mg L^{-1}), P is the observed atmospheric pressure (kPa) and V_P is the saturation vapour pressure of water (kPa). C_{atm} and V_P were estimated as a function of water temperature T (range of application 0-50°C, Demars et al., 2015),

$$C_{atm} = -0.00005858T^3 + 0.007195T^2 - 0.39509T + 14.586 \tag{18}$$

$$V_P = 0.0000802T^3 - 0.000717T^2 + 0.0717T + 0.539 \tag{19}$$

3 Case study

3.1 Study area

The River Otra flows through forests and alpine uplands in the valley of Setesdal and is the largest river in southern Norway. The river drains a catchment area of 4000 km^2 and runs for about 240 km until it meets the North Sea at Kristiansand (Wright et al., 2017). The river is extensively used for hydropower production (about 4 TWh per year) through construction of dams and water transfers, with Brokke being the largest hydropower station in the valley (Rørslett, 1988; Wright et al., 2017).

We applied the models within a 10780 m long river section located downstream of the Brokke hydropower plant (Figure 2). This section drains about 1900 km^2 (Wright et al., 2017). The river stretch can be considered an artificial system with its flow and water level controlled by Brokke hydropower plant at the upstream end and Hekni dam at the downstream end. The oscillating demands on energy production can cause flow to vary from $\sim$ 20-80 m^3 s^{-1} within 24 h under low summer flows. The hydropower plant effluent can also release water highly supersaturated in dissolved gases depending on water intakes (streams *versus* reservoirs) independently of discharge (Pulg et al., 2016). No such supersaturation events were observed during the short term study period here (Demars et al., 2021). In addition to the controlled flow, the river reach also shows profuse growth of the aquatic plant *Juncus bulbosus*, which may create significant amount of water tran-

sient storage, delaying solute transport time relative to the velocity of water (Ensign & Doyle, 2005; Kurz et al., 2017).

Figure 2. Study stretch in the River Otra spanning from Brokke to Hekni. Monitoring locations of river flow (red circle) and dissolved oxygen (black filled circles) are marked on the map.

3.2 Sensor deployment and bathymetry

DO and water temperature were monitored using O_2 and temperature sensors (miniDOT PME) at site 2 (Figure 2). A monitoring station was also installed at site 3 to monitor dissolved oxygen and water temperature (Xylem - Andeeraa optode 4831), photosynthetically-active radiation (LICOR Quantum LI190R-L), air temperature and atmospheric pressure (Barometer RM Young 061302V) using a Campbell data logger (CR1000X). Data from the monitoring station were transferred daily through a Campbell Scientific 4G modem CELL215. Data were logged at 5 min time intervals from 4^{th} (10:00 am) to 8^{th} (15:35) August 2019. The sensor at site 2 was installed vertically facing down in the main current at mid depth, tied to a post. The sensor at site 3 was inserted into a plastic pipe fixed on Straume bridge, and protruded in the main current. The oxygen sensors were cross calibrated in 100% air saturated water in a bucket before and after deployment and small corrections ($< 3\%$ DO saturation) were applied, as previously reported (Demars, 2019).

Total dissolved gas (TDG) was monitored at site 1, 2, 3 and 4 every 30 min at infrequent intervals during a five year period (2012-2017) with Total Gas Analysers 3.0 (Fisch- und Wassertechnik (Pulg et al., 2016) based on the Weiss-saturometer principle (Weiss, 1970). The saturation is measured as the percent dissolved air in the water relative to expectation from ambient air pressure. The saturometer has an accuracy of ± 10 hPa, which is approximately $\pm 1\%$ TDG.

Several thousands georeferenced water depth points were taken throughout the reach with a measuring stick north of Straume and Lowrance sonar in the downstream part to Hekni (Figure A1), and cross calibrated with discharge. Changes in water depth were determined from absolute pressure difference (see Moe & Demars, 2017) between atmospheric pressure and submersible pressure sensors inserted into a perforated plastic tube at sites 1-4 recording at 30 min time intervals (Onset HOBO data loggers U20L-04, accuracy equivalent to 4 mm for water level).

3.3 Flow-velocity

Hourly flow data at Brokke (hydropower plant effluent and river) and Hekni sites were obtained for a duration of 8 days (3/8/2019-10/8/2019) from the hydropower company. Flow observations were not available at Rysstad Øy and Straume, where metabolism

is estimated. Flood wave travel times at these sites were derived from solute travel time using the travel time relationships proposed by Sincock et al. (2003). We used these travel time relationships to back-calculate solute and flow travel time parameters from velocity estimates (Table 1). Velocity estimates in the river reaches were derived using two approaches.

Average velocities for the first section (site 1-2: steep, shallow, fast flowing, cobble bed) were determined using Manning's equation: $v = (1/n)A/{P_m}^{2/3}S_c^{1/2}$, where n is the Manning roughness coefficient (0.04, cobble bed), A is the cross-sectional area of the river channel (m^2), P_m is the wetted perimeter of the river channel (m) and S_c is the channel slope (0.0016 m/m). A and P_m were calculated using changes in water depth. This method could not be applied further downstream due to partial control on water level by Hekni dam.

Average velocities for the second section (site 2-3: very wide, gentle slope, sandy bed) and the third section (site 3-4: narrow, water level controlled by Hekni dam) were estimated from section length (L) and mean travel time (T_s) of large peaks in TDG, where $u_s = L/T_s$. We used cross correlation function in R (Venables & Ripley, 2002) to identify average travel time lags (h) between TDG time-series across the sites. Large TDG super-saturation events (threshold $> 130\%$ at Brokke) with time lag correlation coefficient > 0.4 were selected for the estimation of velocity. These velocities were plotted against discharge at Hekni (averaged for corresponding event duration) to establish flow-velocity relationship for each reach. TDG travel times ranged between 2-12 hours and 7-13 hours in the second (site 2-3) and third sections (site 3-4), respectively. This method could not be applied in the first section as the temporal resolution of the TDG data was too coarse relative to the mean travel time (< 1 h).

We established relationships between flow and TDG velocity as $u_s = bQ^c$ for three discernible sections. Ideally a conservative solute should be used to estimate flow-velocity parameters (b, c). While TDG is not a conservative tracer, the selection of the largest peaks to differentiate from noise and the very low gas exchange rate in these sections gave a similar result to a continuous addition of lime under high flow conditions (about 102 $m^3\ s^{-1}$) monitored with electric conductivity sensors deployed at Straume (site 3) and Hekni (site 4). Power regressions between the velocities of TDG waves and corresponding mean flows at Hekni provided values of constants b and c for the second ($R^2 = 0.78$)

Table 1. Velocity and travel time formulations in the ADV and ADZ models for the River Otra back-calculated based on the travel time relationships proposed by Sincock et al. (2003). (CSTR, continuous stirred tank reactor)

	ADV model	ADZ model
Solute velocity	$u_s = bQ^c$	$u_s = bQ^c$
Solute-lag coefficient	$\beta = 0$	$\beta = 1.55$ (see Appendix)
Mean flow velocity	$u_{adv} = u_s$	$u_{adz} = (1+\beta) \times u_s$
Celerity	$c_{adv} = m \times u_{adv}$	$c_{adz} = m \times u_{adz}$
Water residence time in CSTR	$T_{uadv} = L/u_{adv}$	$T_{uadz} = L/u_{adz}$
Total solute travel time	$T_{sadv} = T_{uadv}$	$T_{sadz} = L/u_s$
Advection delay	$\alpha = F_{adv}T_{sadv}$	$\tau_s = T_{sadz} - T_{uadz}$
Dead zone residence time		$T_{adz} = T_{uadz}$

and third sections ($R^2 = 0.56$) (Figure A2, Table A1). Water travelled fastest in the first section (Brokke-Rysstad Øy) with a mean velocity of 0.73 m s^{-1}, slowest (0.14 m s^{-1}) in the widest section with high plant growth (Rysstad Øy-Straume) and slow-flowing in the narrower and deeper third section (0.27 m s^{-1}) for a 50 m^3 s^{-1} discharge.

3.4 Gas exchange rate

The gas transfer velocity (kz) of CO_2 was estimated as the flux of CO_2 (F_{CO2}, mmol m^{-2} h^{-1}) determined using floating chambers equipped with infra-red gas analysers (following Bastviken et al., 2015) relative to the CO_2 saturation deficit as follows ($C_s - C$, mmol m^{-3}),

$$kz = \frac{F_{CO2}}{C_s - C} \tag{20}$$

More specifically, CO_2 efflux (or influx) were estimated in 33 half-hour runs, from the average of three chambers for each run drifting freely at the water surface and logging at 30 s time intervals. The runs were conducted between March 2020 and August 2020 under varying temperature, discharge and depth. The calculations of CO_2 flux for individual chambers followed Martinsen et al. (2018). Water samples were collected at the beginning and end of each run in 120 mL glass bottles to determine the CO_2 saturation deficit. Water bottles were filled to the rim and capped underwater, then crimped.

Mercuric chloride ($HgCl_2$) was immediately added to stop biological processes (100µL of half saturated solution per 120 mL bottle). The samples were kept cool (+4°C) and in the dark until the day of gas analysis. The samples were warmed and weighed at room temperature, a 30 mL helium headspace was created, the samples were weighed again (to determine the volume of water removed from the bottle), and shaken gently horizontally for at least an hour. The headspace was analysed by gas chromatography and concentrations were calculated following Yang et al. (2015). It was checked that the addition of $HgCl_2$ did not affect the determination of CO_2 (Borges et al., 2019; Koschorreck et al., 2021).

The specific flux F_{CO2} was not related to water temperature, discharge, depth or velocity. Thus $kz = 0.022 \pm 0.004$ m h^{-1} was estimated as the slope of the regression line between specific CO_2 flux and CO_2 saturation deficit (Figure A3). In theory the regression line should go through the origin, but the uncertainties were reasonable given the modest range of dissolved CO_2 saturation (70-267%). Thus, knowing the average depth ($z = 1.82$ m) during the chamber runs, the gas exchange coefficient was calculated for CO_2 as $k_{CO2} = 0.012 \pm 0.002$ h^{-1}.

Finally, the oxygen gas exchange coefficient k_{O2} was simply calculated from $k_{O2} = k_{CO2}/0.81$ (Demars, 2019), where the constant 0.81 accounts for differences in the rates of CO_2 and O_2 diffusion in water independently of temperature (Davidson, 1957). The estimate of k_{O2} (0.35 ± 0.07 d^{-1}) indicated low gas exchange, comparable to other rivers with similar depth-velocity (< 2 d^{-1}, Palumbo & Brown, 2014). k_{O2} was used as a constant in the metabolism models (k in Eq. 6, Eq. 7, Eq. 9) to simulate reaeration flux.

3.5 Model application and parameter estimation

We developed the model code in Python (3.6.3) and it is available on Zenodo repository (Pathak, 2022). Flow and solute dynamics in the river were described using ordinary differential equations, and solved through an accounting method using finite difference approximation and inverse modelling using odeint() function from the `Scipy` package (v1.5.0) in python. The odeint() function solves ordinary differential equations using lsoda solver from the FORTRAN library odepack.

The boundaries of the river network for model implementation were decided based on data availability. The modelling approach presented here requires observations at min-

imum two sites in the river, one for input and one for parameter calibration. The flow routing model was first implemented at 5 min time-steps for the river stretch between Brokke and Hekni since flow hydrographs were available at these two sites. Flows at Rysstad Øy and Straume were then simulated using the optimised parameters between Brokke and Hekni. The solute model was implemented at 5 min time-steps for the river stretch between Rysstad Øy and Straume since oxygen observations were available at these sites. Although the metabolism model implementation in this study is limited to one reach, the model can be extended for multi-reach application (code available by Pathak (2022)).

Model parameters in the inverse model were estimated using a two-step calibration process (similar to Sincock & Lees, 2002), where flow parameters were first optimised with respect to the observed flow, prior to the optimisation of metabolic parameters. Flow parameters can be optimised between the gauging sites on reach-by-reach basis in downstream direction. Flow time-series at Brokke and Hekni were used to first optimise F_r parameter. Flow at Rysstad Øy and Straume were then modelled using the optimised value of F_r.

Solute travel times in the River Otra were derived based on velocities as described in section 3.3 (Table 1). Next, metabolic parameters (P_{GPPmax}, k_{PAR}, R_{ER}) were optimised in the process of fitting oxygen time-series. Model parameters were optimised using a least-squares minimisation approach with the Nelder-Mead algorithm (Gao & Han, 2012) from the `lmfit` package (v1.0.1) in Python. Lower and upper bounds were provided from prior knowledge to constrain the inverse model parameters and avoid parameter equifinality. Initial values of P_{GPP}, k_{PAR} and R_{ER} were provided from the outputs of the two-station accounting method. F_{adv} was optimised in the modified two-station model (ADV formulation, accounting method) by minimising the residual sum of squares of GPP-PAR link function (Eq. 16), and was used as a constant in the inverse ADV model. Metabolism parameters were assumed to be constant over a period of 24 h for a given reach.

We sampled Bayesian posterior distribution of solute model parameters using the Markov Chain Monte Carlo (MCMC) algorithm using the `emcee` package (v3.0.2) in python. This method calculated the log-posterior probability ($ln\, p(\theta_{true}|D)$) of the model parameters (θ) given the data (D),

$$\ln p(\theta_{true}|D) \propto \ln p(\theta_{true}) - \frac{1}{2}\sum_n [\frac{(g_n(\theta_{true}) - D_n)^2}{{S_n}^2} + \ln(2\pi {S_n}^2)] \tag{21}$$

where $ln\,p(\theta_{true})$ is the log-prior. The second term on the right represents log-likelihood, $ln\,p(D|\theta_{true})$, where g_n is the generative model, D_n is the data and S_n is the measurement uncertainty. Note that we did not use the MCMC algorithm for parameter optimisation. Instead, we first optimised the model parameters using the Nelder-Mead algorithm and later used the MCMC algorithm to sample from the posterior distribution of these optimised values to obtain parameter uncertainties and covariance.

4 Results

Performances of flow routing and metabolism models were evaluated separately. River flows were simulated ahead of the metabolism estimation and outputs from the flow routing model were fed as inputs in the metabolism model. An initial visual inspection of flow and DO curves showed that water travelled faster than DO within the study reach (Figure A4). Such a time lag could result either from the dual water regulation at Brokke and Hekni or from the excessive vegetation in the river reach between Rysstad Øy and Straume. Therefore, to account for this time lag, we included both potential causes in the model formulations i.e., pure advection (ADV, Eq. 7) and also including transient storage (ADZ, Eq. 9) for metabolism estimation. In this section, we present the results of the flow routing and metabolism model applications. Furthermore, we provide posterior probability distribution of optimised model parameters in the inverse metabolism model.

4.1 Influence of hydropower plant on DO dynamics along the reach

The O_2 turnover in the second section (site 2-3) was only 14%, calculated as $O_{2,\text{turnover}} = 1-1/exp(kL/u)$ (rearranged oxygen footprint equation, Demars et al., 2015), where L = reach length (4660 m), u = average water velocity (8.03 m min^{-1}) and k = reaeration coefficient (0.00025 min^{-1}). The output suggests that 86% of the oxygen variability at Straume (site 3) can be attributed to the variability of oxygen at Rysstad Øy (site 2). It is known that the hydropower plant affects greatly total dissolved gas variation at Rysstad Øy (Pulg et al., 2016). Hence, the conventional one-station model (Odum, 1956; Appling, Hall Jr, et al., 2018) or averaged two-station model (Demars et al., 2011; Demars, 2019) would not provide reliable metabolism estimates in the study section. It also highlights the difficulty of the task of disentangling metabolism from background noise, notably the hy-

dropower plant effluent at Brokke representing 87% of median flow i.e., most of the O_2 mass flux.

4.2 Flow routing model

The flow routing model was able to capture the timing and magnitude of flow peaks and troughs (Figure 3). The model estimated average 61% retention for flow in the river stretch ($F_r = 0.61$). Minor discrepancies between modelled and observed flows were expected because the flow routing model does not account for the effect of flow regulation at the downstream (Hekni) end that causes rapid rises and falls in water level at Hekni. Nevertheless, the flow routing model satisfactorily reproduced flow variation at Hekni with goodness-of-fit (R^2) of 0.87 (Figure 3b).

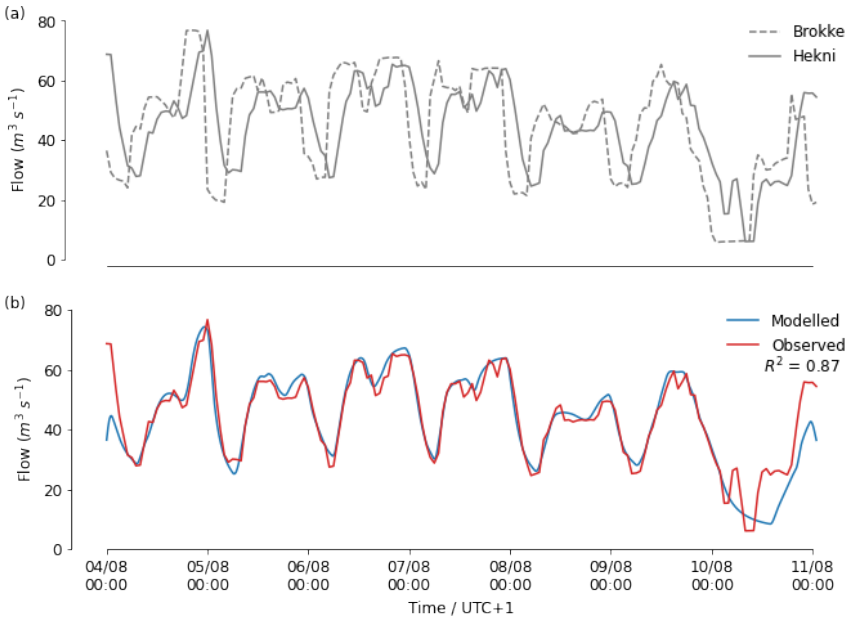

Figure 3. Comparison of flow observations at Brokke and Hekni sites (a) and modelled and observed flows at Hekni site (b) at 5 min time-steps

4.3 Modified two-station model (accounting method)

Modified two-station model formulation with only pure advection (ADV) performed better than the formulation with pure advection plus transient storage (ADZ) (Figure 4). The two-station ADZ model simulated sudden drops in NEP at Straume around mid-day, suggesting a sudden decrease in GPP around mid-day since ER was assumed to be

constant. Variation in PAR did not explain the mid-day drops in GPP (Figure 4c). While an afternoon lull in GPP has often been reported, the estimated mid-day drops in NEP were not driven by biological production, but indicated a systematic error in the metabolism estimates resulting from errors in the simulation of DO mass flux. The mass flux of DO in the river largely followed flow variation. The upstream site (Rysstad Øy) showed concurrent decline in flow and DO in the afternoon owing to changing water demand for power plant operations (Figure A4). The downstream site (Straume) did not show a concurrent decline in DO and flow, but showed shoulders in the DO time-series earlier in the day (around mid-day). These shoulders result from delayed transport of DO from Rysstad Øy to Straume (Figure A4) since oxygen variation at Straume is highly influenced by oxygen variation at Rysstad Øy (explained in section 4.1). Although the two-station ADZ model accounts for these delayed transport mechanisms through transient storage influence, the model was unable to model NEP variation accurately. The ADV model, on the other hand, was able to resolve the issue of mid-day drops in GPP to a larger extent.

Both models showed a positive relationship between photosynthesis and light, with saturation of photosynthesis under high light intensity (Figure 4). The ADV model ($R^2 = 0.56$, Figure 4a) represented a slightly better regression fit than the ADZ model ($R^2 = 0.44$, Figure 4b) for GPP-PAR link function (Eq. 16). The estimates of half-saturation light intensity in both models (Figure 4) were in line with what is commonly observed in freshwater systems (k_{PAR} = 100-500 µ mol quanta m^{-2} s^{-1}, Demars et al., 2011). The estimates of P_{GPPmax} and k_{PAR} fitted in the GPP-PAR link function (Figure 4) served as priors in the inverse model when simulating GPP as a function of PAR.

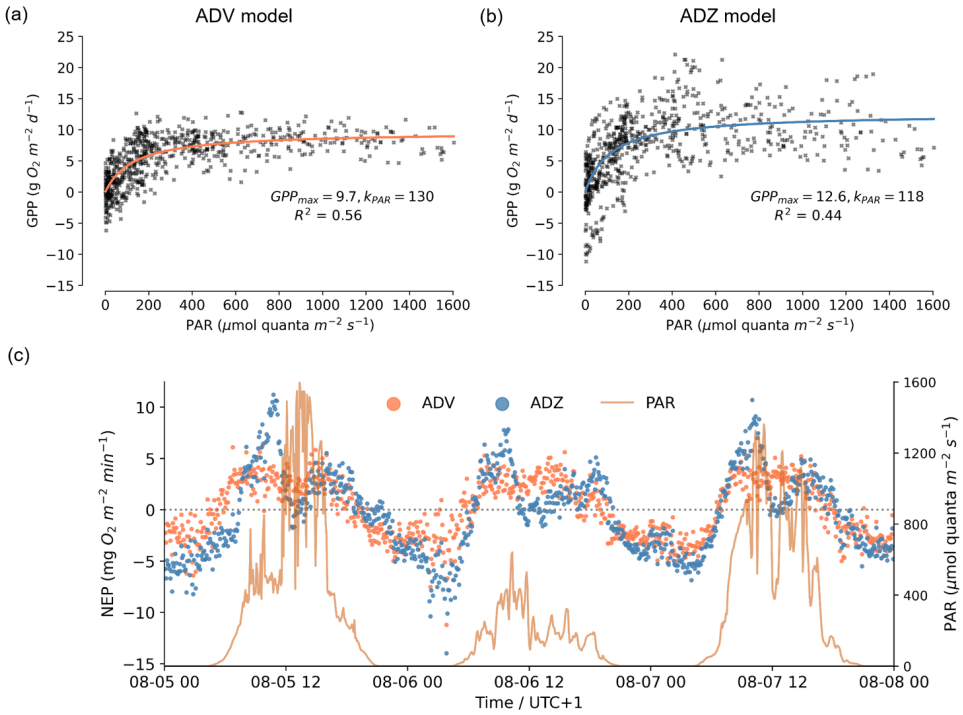

Figure 4. Non-linear regression between gross primary production (GPP) and photosynthetically-active radiation (PAR) in the modified two-station (a) ADV and (b) ADZ models at Straume. (c) shows the variation in net ecosystem production (NEP) and PAR in the modified two-station models at Straume.

4.4 Inverse metabolism model

Both ADV and ADZ formulations captured the overall DO variation at Straume (Figure 5), but the ADV model performed significantly better than the ADZ model to capture the overall trend and magnitude of oxygen variation. The ADZ model showed a small time lag between the observed and modelled DO concentrations, which indicates inaccuracies in the simulation of DO mass flux with flow. Note that the flow-velocity relationships derived for TDG in the study reach does not cover the entire range of observed flows during the modelling period (e.g. equations derived for velocities at Q $>$ 50 m^3 s^{-1} for reach 2, Figure A2).

Estimated values of metabolism parameters in the ADV model are generally lower than the estimates of the ADZ model (Table A2). The ADV model ($R^2 = 0.96$) derived a better overall goodness-of-fit than the ADZ model ($R^2 = 0.83$). Therefore, we selected

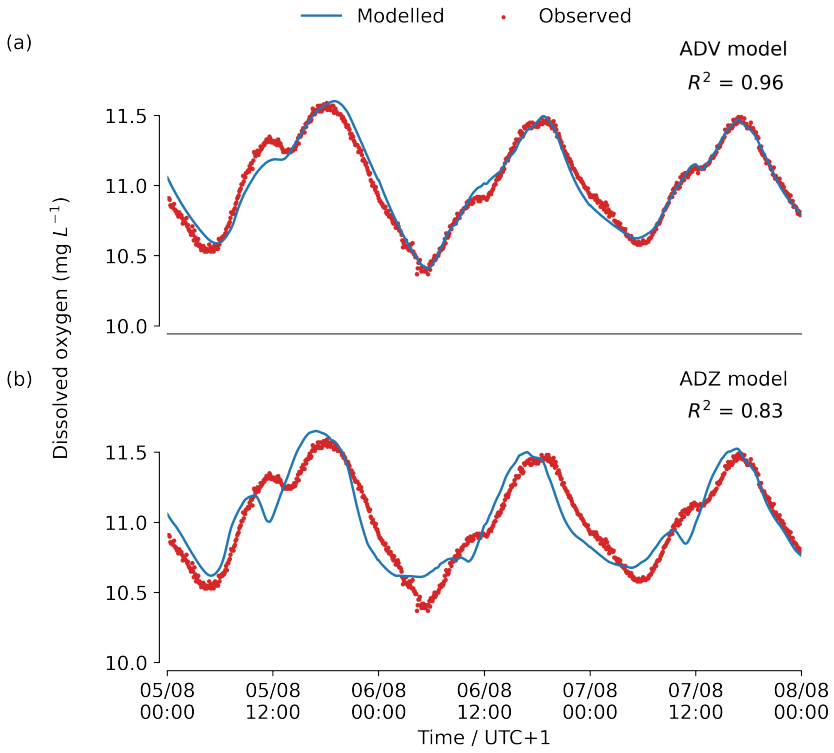

Figure 5. Comparison of modelled and observed dissolved oxygen concentrations at 5 min time-steps at Straume in the inverse (a) ADV and (b) ADZ formulations

the ADV model to sample Bayesian posterior distribution of metabolism parameters using the MCMC algorithm. P_{GPPmax} and R_{ER} parameters showed a strong positive correlation during the first two days of the modelling period (> 0.86). Other significant correlations were observed between k_{PAR}-P_{GPPmax} (0.95) and k_{PAR}-R_{ER} (-0.63) on the third day. Despite these high correlations, we find that the median values (and maximum likelihood estimates) of all metabolism parameters lie in a close range of the values optimised by the Nelder-Mead minimisation algorithm (within 1-σ uncertainty) (Table 2, Figure 6). The performance of the MCMC algorithm was judged using the estimate of average acceptance fraction, which was found to be within an acceptable range (0.2-0.5, Foreman-Mackey et al., 2013) in all cases. Figure 7 shows the variation in NEP and the relationship between GPP-PAR as estimated in the inverse ADV model.

Table 2. Median values of posterior probability distribution of the inverse ADV model parameters with 1-σ uncertainty derived from the MCMC runs and optimised parameter values by the Nelder-Mead least-squares minimisation algorithm (in brackets). Units are g O_2 m^{-2} d^{-1} for P_{GPPmax} and R_{ER}, and µmol quanta m^{-2} s^{-1} for k_{PAR}.

Parameter	Day 1	Day 2	Day 3
P_{GPPmax}	8.64±0.16 (8.64)	12.38±0.12 (12.96)	11.52±0.24 (11.52)
k_{PAR}	144±5 (144)	144±1 (144)	461±32 (461)
R_{ER}	3.46±0.09 (3.46)	4.61±0.05 (4.32)	4.03±0.04 (4.03)

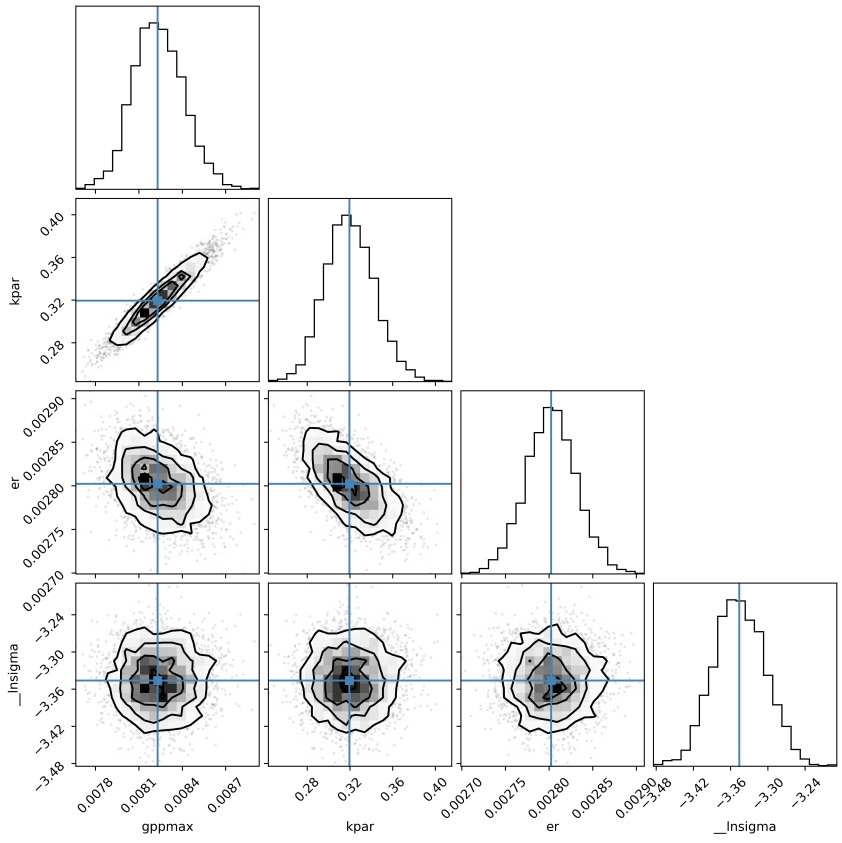

Figure 6. Posterior distribution of inverse ADV model parameters gppmax (P_{GPPmax}), kpar (k_{PAR}) and er (R_{ER}) using MCMC algorithm on day 3. Blue lines show the median values of posterior probability distribution of model parameters. _lnsigma parameter is used to estimate the true uncertainty in the data.

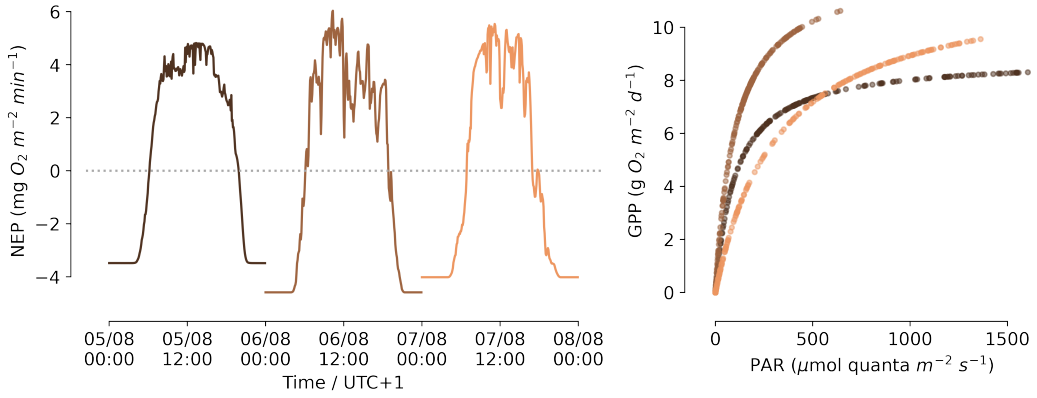

Figure 7. Estimated net ecosystem production (NEP) (a) and modelled GPP-PAR relationship (b) at Straume in the inverse ADV model. GPP = gross primary production and PAR = photosynthetically-active radiation.

5 Discussion

The MUFT model application here demonstrates how the impact of hydropeaking (i.e. sub-daily flow fluctuations) and transient storage can be included in the estimation of metabolism. The better performance of the ADV model compared to the ADZ model here suggests that despite the initial hypothesis, river vegetation may not produce significant transient storage (ADZ) and that introduction of pure transportation delay (ADV) in the model may be sufficient to characterise DO dynamics at Straume during the modelling period. However, due to limited data availability, it is difficult to confidently pinpoint the dominant transport mechanism in the river. Since, the aim of this study is to present a general model application for metabolism estimation, we do not delve in to the specifics of the process-dynamics in the River Otra. In this section, we discuss the differences in the inverse and accounting modelling approaches along with their limitations and the possibilities of future model improvements.

5.1 Comparison of the inverse model with the modified two-station model

Discrepancies in the outputs of the inverse and modified two-station models mainly arise from the differences in the model structures. For example, the numerical solution of the ODE equation in the modified two-station model uses a simple Euler finite difference scheme as opposed to a more robust lsoda solver from the FORTRAN library ode-

pack (Hindmarsh, 1983) in the inverse model. Moreover, both models characterise GPP in different ways. The accounting approach, although advantageous for not assuming the type of relationship between GPP and PAR, may fail to segregate the influence of flow on DO mass flux from the influence of biological production on DO transformations, when DO mass flux and/or solute-lag coefficient are not characterised accurately. On the other hand, the inverse model is able to segregate these influences up to a certain extent because GPP is modelled as a function of PAR.

Another difference between the two approaches is the parameter calibration process. The two-station method involves an accounting approach where NEP is directly estimated from oxygen observations without any parameter calibration procedure. Daily average ER is then estimated during dark hours, and GPP is calculated as a difference between NEP and daily average ER. The inverse model, on the other hand, optimises model parameters in the process of fitting modelled DO to observed DO time-series using a least-squares minimisation algorithm; hence, providing more confidence in the model estimates. Admittedly, the inverse approach includes more number of model parameters, corresponding to a larger number of degrees of freedom and consequently, the risk of parameter equifinality (Spear & Hornberger, 1980). However, as demonstrated in this study, equifinality may be reduced by constraining the parameter space with prior knowledge of the river system and by minimising the number of unknown parameters by using field measurements to the extent feasible (e.g. Du et al., 2014). Often, random sampling methods such as MCMC algorithms are useful to estimate uncertainty in the optimised model parameters (e.g. Segatto et al., 2021) as represented in this study. Furthermore, sensitivity analysis may also be used to identify the most influential parameters for the simulations (e.g. Vandenberghe et al., 2001).

Although the modified two-station approach is simpler and quicker compared to the inverse model, its application is limited to a much smaller spatial scale, i.e. river-reach scale. Additionally, the two-station accounting approach relies on continuous DO measurements at both sites in the river reach of interest, which is often not possible due to adverse field conditions, drifting of sensors, etc. (Wagner et al., 2006). On the contrary, the inverse model is an apt alternative to estimate long-term trends in metabolism at a river-network scale even when there are gaps present in continuous DO measurements at calibration sites. Despite the differences laid out here, we showed that the outcomes from the two-station accounting approach are useful to constrain the metabolism

parameters in the inverse model. Therefore, both approaches are complementary rather than competitive.

5.2 Modelling limitations and future efforts

The parsimonious model MUFT relies on certain assumptions. For example, the flow routing model approximates constant flow parameters for the entire reach between Brokke and Hekni because it employs reach-by-reach calibration method between gauging stations. In this study, a constant retention parameter was assumed for the entire river section between Brokke and Hekni. This assumption is not realistic since river hydraulics vary within the stretch (discussed in section 3.3). Although we accounted for heterogeneity using reach-wise flow-velocity relationships in the flow routing model, such data may not be easily available in other rivers. It is important to estimate flow parameters precisely because small errors in flow parameters may result in large errors in metabolism estimates when flow dominates the mass flux of oxygen in the river. Multiple non-linear storage tanks ($n_c > 1$) may be more appropriate when the river section is heterogeneous, but increasing n_c value did not significantly improve model performance in this case. Parameter sensitivity analysis (e.g. Sincock et al., 2003) may also be employed prior to MCMC simulations to identify an appropriate model structure and reduce bias in the flow parameters. However, a more detailed investigation of parameter bias is out of the scope of this study.

It is difficult to derive a physical understanding of travel time mechanisms because of the lumped parameter structure of the MUFT model. Characterisation of oxygen travel time from flow based parameters integrates flow and metabolism models and therefore, overcomes this issue to a certain extent. However, it is still difficult to relate travel time parameters to river hydraulic properties and interpret the physical significance of model coefficients because of the crude description of dead zone (ADZ, Wallis et al., 1989) and advective transport (ADV, Beck, 1976) in the model. For example, we found ADZ residence time to be poorly related to metabolism. A lack of strong relationship may partly be attributed to the assumption that TDG velocity $\approx$ solute velocity in the river. This assumption may introduce some bias in NEP estimates. Conservative tracer experiment may help characterise solute travel time parameters (e.g. T_{sadz}, T_{adz}, β) more accurately and consequently, help reduce the bias in metabolism estimates. A poor relationship may also occur from model's inability to account for the diversity of transient storage com-

ponents that contribute to different metabolic processes (e.g. autotrophic and heterotrophic production) (Haggerty et al., 2009). One way to account for diverse transient storage zones is through resazurin tracer experiments, to segregate metabolically active transient storage from a less-active transient storage (Haggerty et al., 2009; Argerich et al., 2011). However, the possibility of a weak or non-existent relationship between transient storage and ecosystem functioning cannot be neglected (Bernhardt et al., 2002; Webster et al., 2003). Nonetheless, in spite of limited available data and a simplified structure, both formulations of the model are able to provide fairly accurate predictions of oxygen transport and dispersion in this as well as previous studies (Lees et al., 2000; Santos Santos & Camacho, 2022). The MUFT model thus offers an alternative with a trade-off between accuracy and complexity.

Another simplification in the MUFT model is in the way in-stream processes are modelled. The ADZ formulation, in particular, assumes that metabolic activity occurs in the transient storage zone, and not during oxygen advection. Lees et al. (1998) proposed a mass decay term for non-conservative solutes (e.g. ammonium). However, it is difficult to characterise mass decay of oxygen during advection through a single term, when coupled with stream metabolism approach. On the other hand, the ADV formulation does not have this issue since it assumes that advection process is dominant in the river reach. The model also includes a simple formulation of metabolism fluxes, but a more complex formulation may be included if necessary. We find that a Michaelis-Menten type equation adequately simulates GPP in the River Otra, but the model can be easily modified to include other formulations such as linear (Payn et al., 2017) or hyperbolic tangent function (Holtgrieve et al., 2010; Jassby & Platt, 1976). We assume constant ER over a day to keep the model structure simple, but ER may be varied as a function of water temperature (Holtgrieve et al., 2010; Song et al., 2018) if deemed necessary in the river system. Estimate of gas-exchange coefficient k is crucial since a small bias in k may lead to a large bias in metabolism estimates (Hall Jr & Ulseth, 2020). k may be modelled as a function of river hydraulic properties (Raymond et al., 2012) or may be estimated during model calibration with prior information from empirical relationships or direct measurements (Holtgrieve et al., 2010). Here, k is estimated from floating chamber studies, performed under a limited range of flows. Use of a constant k value during the modelling period was adequate in this case because the study reach repre-

sented slow-flowing water with considerably low gas-exchange compared to metabolism, thus limiting biases in metabolism from biases in k.

In the River Otra, we find that both inverse modelling approaches are able to predict oxygen variation in the study reach, although performance of the ADV model is significantly better than the ADZ model. The MUFT modelling approach presents opportunities to estimate metabolism in rivers with unsteady flows and/or transient storage zones. Popular approaches of solute modelling with unsteady flows (e.g. flood routing models based on Saint-Venant equations) or including transient storage zone effects with steady flows (Bencala & Walters, 1983; Manson et al., 2010; Runkel, 1998) use partial differential equations (one-dimensional) to simulate water and solute movement. The MUFT model, on the other hand, takes a simpler approach by characterising river reaches as non-linear storage zones in series (zero-dimensional), and simulates water and solute movement using ordinary differential equations. Due to its parsimonious structure, the model includes fewer calibration parameters. Furthermore, the model offers flexibility in selecting an appropriate formulation (e.g. unsteady flows, solute transport mechanisms) that best represents the river conditions.

6 Summary and conclusion

This study presents a coupled modelling approach (MUFT) to estimate whole-stream metabolism in rivers with unsteady flow conditions and transient storage zones. The MUFT model integrates flow and oxygen modelling based on travel-time relationships proposed by Sincock and Lees (2002), which were originally built on QUASAR (Whitehead et al., 1997) and ADZ (Lees et al., 2000; Wallis et al., 1989) model equations. We propose an additional model formulation for dominant advective transport (ADV) based on the model developed by Beck and Young (1975). The MUFT approach can be applied through inverse modelling or accounting method (two-station method) according to user's preference and data availability. We demonstrated the application of the MUFT model in the River Otra in southern Norway. We found that the accounting method is simpler, but shows high bias in metabolism estimates when oxygen mass flux is not precisely modelled. The inverse modelling approach is more robust as it employs least-squares minimisation algorithm to optimise model parameters. Moreover, the inverse model supports investigation of parameter uncertainties and correlations through Bayesian sampling of posterior distributions.

The MUFT approach presents opportunities to estimate whole-stream metabolism in hydropeaking river environments as well as in rivers influenced by transient storage zones. With increasing feasibility of high-resolution, long-term oxygen monitoring in rivers (Appling, Hall Jr, et al., 2018; Appling, Read, et al., 2018; Bernhardt et al., 2022), it is possible to extend the model for network-scale metabolism prediction. Using the knowledge of river hydraulics, the inverse model may also be able to predict metabolism rates at sites within the river network where continuous monitoring is not carried out (e.g. Pathak et al., 2022). In future, the model can be implemented for metabolism prediction under changes such as warming, extreme weather events and river management practices - a research area that calls for more attention (Bernhardt et al., 2018).

Appendix A Appendix

A1 Estimation of solute-lag coefficient

Using average TDG travel time (Table A1), $m = 5/3$ (Chapra, 2008) and average flood wave travel time in Eq. A1, $\beta = 1.55$ is derived for the river section between Brokke and Hekni.

$$m = \frac{c}{u} = \frac{c}{u_s \times (1+\beta)} = \frac{\frac{10780}{190}}{\frac{10780}{807} \times (1+\beta)} \tag{A1}$$

A2 Estimation of flow routing parameters

Flood wave travel time T_{flow} can be dervied from reach length and avereage celerity as shown in Eq. 2. Based on Eq. 2 and travel time relationships provided in Table 1,

$$T_{flow} = \frac{L}{c} = \frac{L}{m(1+\beta)u_s} \tag{A2}$$

Solute travel time (T_s) at time t for a reach i is expresses as,

$$T_s = \frac{L_i}{u_s} = \frac{L_i}{b_i Q_t^{c_i}} \tag{A3}$$

Substituting Eq. A3 in Eq. A2,

$$T_{flow} = \frac{\frac{L_1}{b_1 Q_t^{c1}} + \frac{L_1}{b_2 Q_t^{c2}} + \frac{L_3}{b_1 Q_t^{c3}}}{m(1+\beta)} \quad \text{(A4)}$$

Values of b and c constants for each reach are provided in Table A1.

A3 Model application and outputs

Table A1. Description of river reaches (L = length, W = mean width, v = velocity, τ = travel time)

Reach no	Reach name	L (m)	W (m)	b	c	Mean v (m s^{-1})	Mean τ (min)
1	Brokke - Rysstad Øy	3130	107	0.1554	0.3967	0.73	71
2	Rysstad Øy – Straume	4660	316	0.0047	0.8699	0.14	550
3	Straume - Hekni	2990	119	0.0489	0.4352	0.27	186

Table A2. Parameter values in the inverse ADV and ADZ models optimised using the Nelder-Mead algorithm. Units are g O_2 m^{-2} d^{-1} for P_{GPPmax} and R_{ER}, and µmol quanta m^{-2} s^{-1} for k_{PAR}.

Model	Parameter	Day 1	Day 2	Day 3
ADV	P_{GPPmax}	8.64	12.96	11.52
	k_{PAR}	144	144	460
	R_{ER}	3.46	4.32	4.03
ADZ	P_{GPPmax}	13.82	14.40	12.53
	k_{PAR}	144	144	173
	R_{ER}	6.48	6.48	5.90

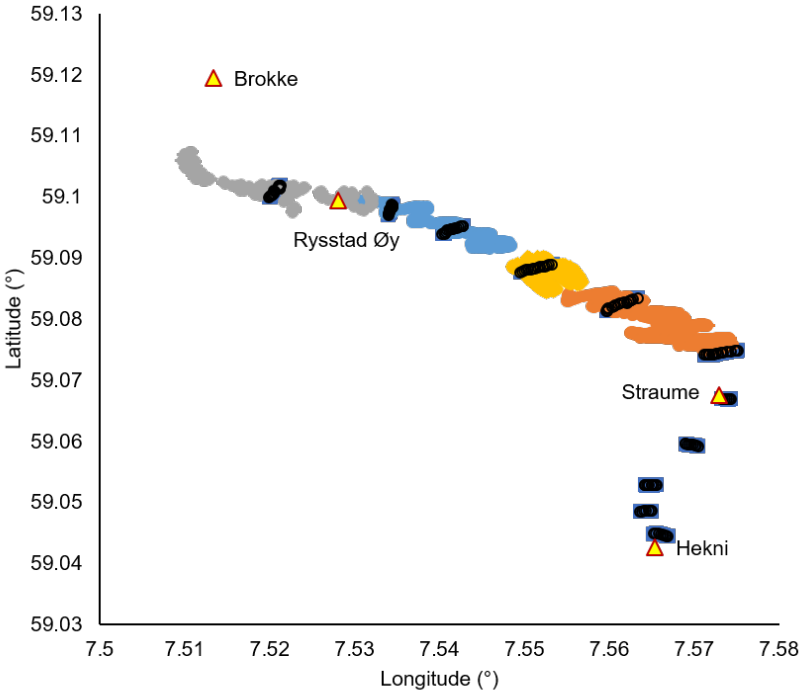

Figure A1. Spatial distribution of depth measurements in the Otra River. Data points are represented with different colours to segregate depths taken on different days during June, 2020. The triangle markers highlight the locations of the gauging sites in the catchment (see Fig 2)

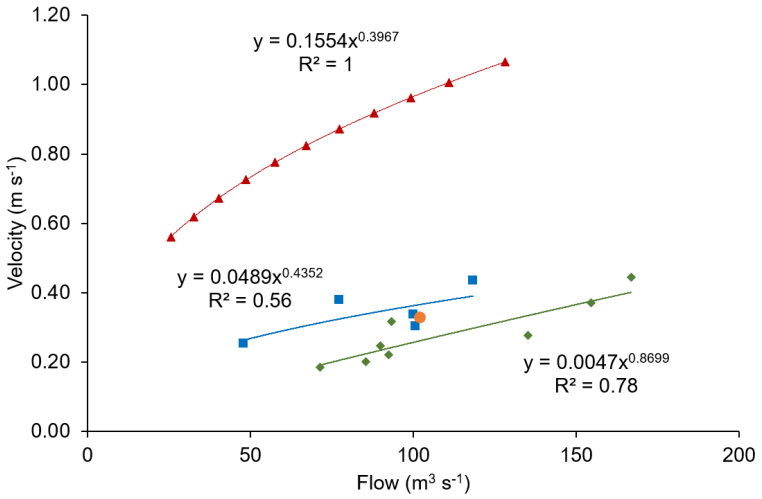

Figure A2. Flow-velocity relationship for reach 1 (maroon, triangle markers), reach 2 (green, diamond markers) and reach 3 (blue, square markers) derived using total dissolved gas observations. Point in orange (circle marker) represents average velocity for a flow of 102 m^3 s^{-1} derived from a lime addition study between Straume and Hekni.

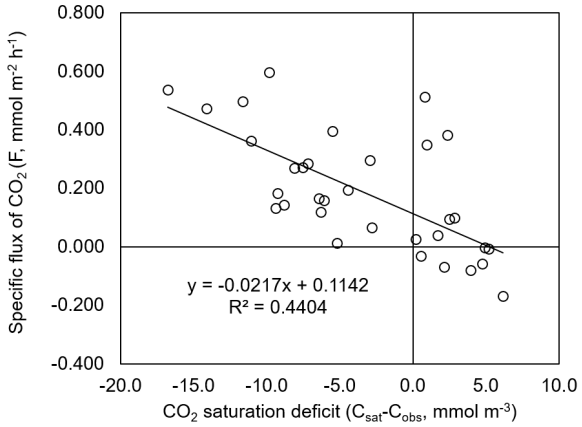

Figure A3. Estimation of gas transfer velocity from a regression between specific flux of CO_2 derived from the floating chamber runs and CO_2 saturation deficit derived from the gas chromatograph analyses

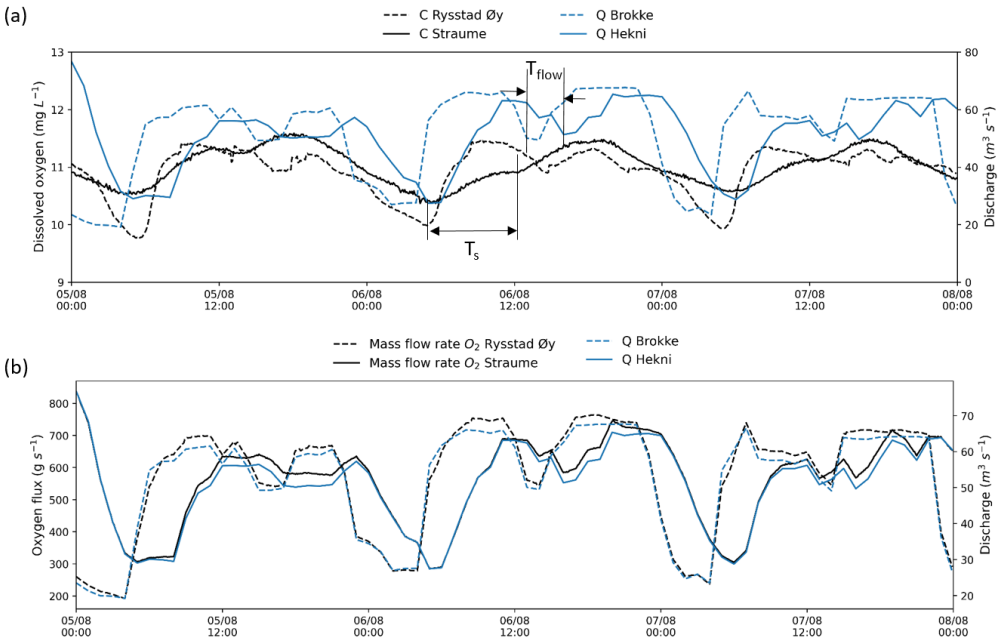

Figure A4. Time-series of observed dissolved oxygen concentrations C and observed flow Q (a) and time-series of observed mass flow rate of oxygen and observed flow Q at sites within the study stretch (b)

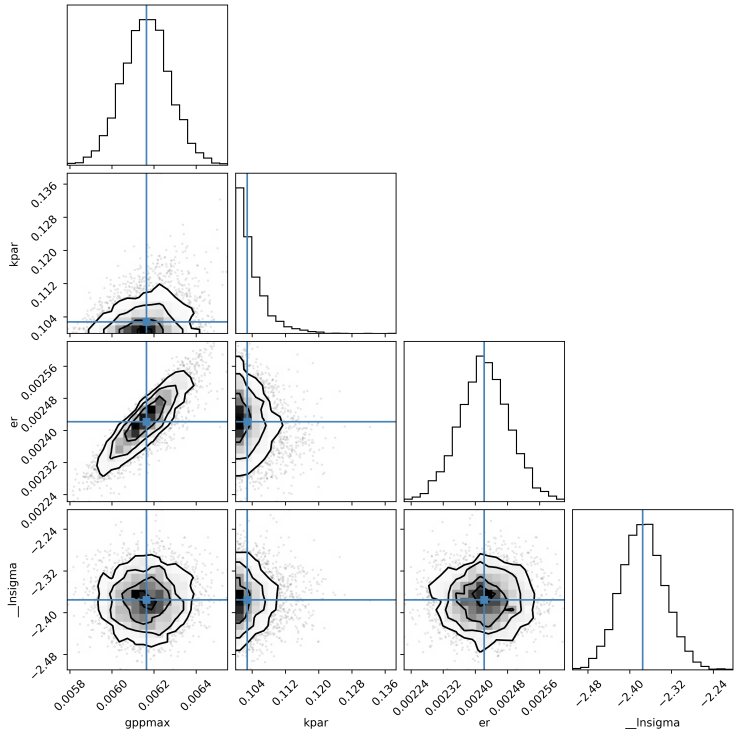

Figure A5. Day 1. Posterior distribution of inverse ADV model parameters gppmax (P_{GPPmax}), kpar (k_{PAR}) and er (R_{ER}) using MCMC algorithm. Blue lines show the median values of posterior probability distribution of model parameters. _lnsigma parameter is used to estimate the true uncertainty in the data.

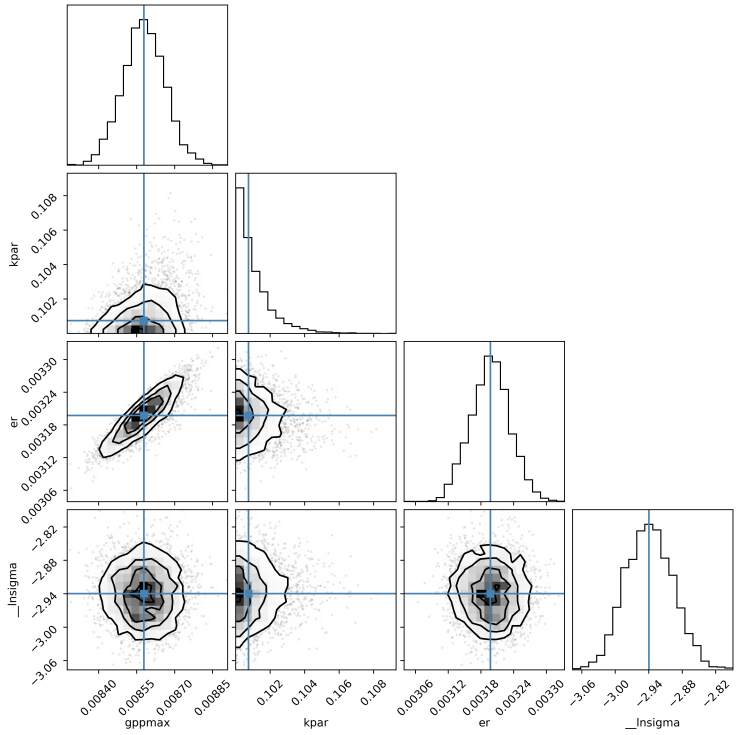

Figure A6. Day 2. Posterior distribution of inverse ADV model parameters gppmax (P_{GPPmax}), kpar (k_{PAR}) and er (R_{ER}) using MCMC algorithm. Blue lines show the median values of posterior probability distribution of model parameters. _lnsigma parameter is used to estimate the true uncertainty in the data.

Acknowledgments

We thank Otra Kraft for providing flow data and boats; Ulrich Pulg and Sebastian Stranzl for providing TDG data and lime addition data; Peter Dörsch for CO_2 GC analyses; Odd Arne Skogan for setting up the Campbell logging station; Knut Olav Oppstad for providing sonar bathymetric data; Kirstine Thiemer, Susanne Schneider, Emmanuel Bergan, Astrid Torske, Eirin Aasland for help collecting bathymetric and plant data, as well as CO_2 flux with the floating chambers. BOLD gratefully acknowledge the Research Council of Norway (297202/E10), the German Federal Ministry of Education and Research (033WU005), the French Agence National de Recherche (N°ANR-18-IC4W-0004-06) and the South African Water Research Commission (K5/2951) for funding of MadMacs (Mass development of aquatic macrophytes - causes and consequences of macrophyte removal for ecosystem structure, function, and services) in the frame of the collaborative inter-

national consortium of the 2017 call of the Water Challenges for a Changing World Joint Programme Initiative (Water JPI). Additional funding was provided by Krypsiv på Sørlandet and the Norwegian institute for water research (NIVA). DP acknowledges the funding from the European Union's Horizon 2020 research and innovation programme under the Marie Skłodowska-Curie grant agreement no. 765553.

Open Research

v0.1.0 of the MUFT model developed for metabolism estimation and data used in the model development and application are preserved at `https://doi.org/10.5281/zenodo.7197544`, available via Creative Commons Attribution 4.0 International license and developed at `https://github.com/d-pathak/MUFT-model/tree/v0.1.0` (Pathak, 2022).

References

Appling, A. P., Hall Jr, R. O., Yackulic, C. B., & Arroita, M. (2018). Overcoming equifinality: Leveraging long time series for stream metabolism estimation. *Journal of Geophysical Research: Biogeosciences*, *123*(2), 624–645.

Appling, A. P., Read, J. S., Winslow, L. A., Arroita, M., Bernhardt, E. S., Griffiths, N. A., ... others (2018). The metabolic regimes of 356 rivers in the united states. *Scientific data*, *5*(1), 1–14.

Argerich, A., Haggerty, R., Martí, E., Sabater, F., & Zarnetske, J. (2011). Quantification of metabolically active transient storage (mats) in two reaches with contrasting transient storage and ecosystem respiration. *Journal of Geophysical Research: Biogeosciences*, *116*(G3).

Aristi, I., Arroita, M., Larrañaga, A., Ponsatí, L., Sabater, S., von Schiller, D., ... Acuña, V. (2014). Flow regulation by dams affects ecosystem metabolism in mediterranean rivers. *Freshwater biology*, *59*(9), 1816–1829.

Ashraf, F. B., Haghighi, A. T., Riml, J., Alfredsen, K., Koskela, J. J., Kløve, B., & Marttila, H. (2018). Changes in short term river flow regulation and hydropeaking in nordic rivers. *Scientific reports*, *8*(1), 1–12.

Bastviken, D., Sundgren, I., Natchimuthu, S., Reyier, H., & Gålfalk, M. (2015). Cost-efficient approaches to measure carbon dioxide (co 2) fluxes and concentrations in terrestrial and aquatic environments using mini loggers. *Biogeosciences*, *12*(12), 3849–3859.

Beck, M. (1976). Dynamic modelling and control applications in water quality main-

tenance. *Water Research*, *10*(7), 575–595.

Beck, M., & Young, P. C. (1975). A dynamic model for do—bod relationships in a non-tidal stream. *Water Research*, *9*(9), 769–776.

Beer, T., & Young, P. C. (1983). Longitudinal dispersion in natural streams. *Journal of environmental engineering*, *109*(5), 1049-1067.

Bencala, K. E., & Walters, R. (1983). Simulation of solute transport in a mountain pool-and-riffle stream-a transient storage model. *Water Resources Research*, *19*, 718–724.

Bernhardt, E. S., Hall Jr, R. O., & Likens, G. E. (2002). Whole-system estimates of nitrification and nitrate uptake in streams of the hubbard brook experimental forest. *Ecosystems*, *5*(5), 419–430.

Bernhardt, E. S., Heffernan, J. B., Grimm, N. B., Stanley, E. H., Harvey, J., Arroita, M., ... Hall Jr, R. (2018). The metabolic regimes of flowing waters. *Limnology and Oceanography*, *63*(S1), S99-S118.

Bernhardt, E. S., Savoy, P., Vlah, M. J., Appling, A. P., Koenig, L. E., Hall, R. O., ... others (2022). Light and flow regimes regulate the metabolism of rivers. *Proceedings of the National Academy of Sciences*, *119*(8).

Borges, A. V., Darchambeau, F., Lambert, T., Morana, C., Allen, G. H., Tambwe, E., ... others (2019). Variations in dissolved greenhouse gases (co 2, ch 4, n 2 o) in the congo river network overwhelmingly driven by fluvial-wetland connectivity. *Biogeosciences*, *16*(19), 3801–3834.

Bottacin-Busolin, A., Singer, G., Zaramella, M., Battin, T. J., & Marion, A. (2009). Effects of streambed morphology and biofilm growth on the transient storage of solutes. *Environmental science & technology*, *43*(19), 7337–7342.

Chapra, S. C. (2008). *Surface water-quality modeling*. Waveland press.

Chapra, S. C., & Runkel, R. L. (1999). Modeling impact of storage zones on stream dissolved oxygen. *Journal of Environmental Engineering*, *125*(5), 415–419.

Chowanski, K., Kunza, L., Hoffman, G., Genzoli, L., & Stickney, E. (2020). River management alters ecosystem metabolism in a large oligotrophic river. *Freshwater Science*, *39*(3), 534–548.

Cimorelli, L., Cozzolino, L., D'Aniello, A., Morlando, F., Pianese, D., & Singh, V. (2016). A new semi-lagrangian routing procedure for constituent transport in steady and unsteady flow velocity fields. *Journal of Hydrology*, *538*, 216–230.

Cox, B. (2003a). A review of currently available in-stream water-quality models and their applicability for simulating dissolved oxygen in lowland rivers. *Science of the total environment*, *314*, 335–377.

Cox, B. (2003b). A review of dissolved oxygen modelling techniques for lowland rivers. *Science of the Total Environment*, *314*, 303–334.

Davidson, J. (1957). The determination of diffusion coefficient for sparingly soluble gases in liquids. *Trans. Instn Chem. Engrs.*, *35*, 51–60.

Demars, B. O. L. (2019). Hydrological pulses and burning of dissolved organic carbon by stream respiration. *Limnology and Oceanography*, *64*(1), 406–421.

Demars, B. O. L., Dörsch, P., Thiemer, K., Clayer, F., Schneider, S. C., Stranzl, S. F., ... Velle, G. (2021). *Hydropower: gas supersaturation and the role of aquatic plant photosynthesis for fish health* (Tech. Rep. No. 7633-2021). Norwegian Institute for Water Research.

Demars, B. O. L., Gíslason, G. M., Ólafsson, J. S., Manson, J. R., Friberg, N., Hood, J. M., ... Freitag, T. E. (2016). Impact of warming on co 2 emissions from streams countered by aquatic photosynthesis. *Nature Geoscience*, *9*(10), 758–761.

Demars, B. O. L., Russell Manson, J., Olafsson, J. S., Gislason, G. M., Gudmundsdottír, R., Woodward, G., ... Friberg, N. (2011). Temperature and the metabolic balance of streams. *Freshwater Biology*, *56*(6), 1106-1121.

Demars, B. O. L., Thompson, J., & Manson, J. R. (2015). Stream metabolism and the open diel oxygen method: Principles, practice, and perspectives. *Limnology and Oceanography: Methods*, *13*(7), 356-374.

Du, E., Link, T. E., Gravelle, J. A., & Hubbart, J. A. (2014). Validation and sensitivity test of the distributed hydrology soil-vegetation model (dhsvm) in a forested mountain watershed. *Hydrological processes*, *28*(26), 6196–6210.

Ensign, S. H., & Doyle, M. W. (2005). In-channel transient storage and associated nutrient retention: Evidence from experimental manipulations. *Limnology and Oceanography*, *50*(6), 1740-1751.

Fellows, C. S., Valett, M. H., & Dahm, C. N. (2001). Whole-stream metabolism in two montane streams: Contribution of the hyporheic zone. *Limnology and Oceanography*, *46*(3), 523-531.

Ferreira, V., Elosegi, A., D Tiegs, S., von Schiller, D., & Young, R. (2020). Or-

ganic matter decomposition and ecosystem metabolism as tools to assess the functional integrity of streams and rivers–a systematic review. *Water*, *12*(12), 3523.

Foreman-Mackey, D., Hogg, D. W., Lang, D., & Goodman, J. (2013). emcee: the mcmc hammer. *Publications of the Astronomical Society of the Pacific*, *125*(925), 306.

Gao, F., & Han, L. (2012). Implementing the nelder-mead simplex algorithm with adaptive parameters. *Computational Optimization and Applications*, *51*(1), 259-277.

Haggerty, R., Martí, E., Argerich, A., Von Schiller, D., & Grimm, N. B. (2009). Resazurin as a "smart" tracer for quantifying metabolically active transient storage in stream ecosystems. *Journal of Geophysical Research: Biogeosciences*, *114*(G3).

Hall, R. O., Tank, J. L., Baker, M. A., Rosi-Marshall, E. J., & Hotchkiss, E. R. (2016). Metabolism, gas exchange, and carbon spiraling in rivers. *Ecosystems*, *19*(1), 73–86.

Hall Jr, R. O., & Ulseth, A. J. (2020). Gas exchange in streams and rivers. *Wiley Interdisciplinary Reviews: Water*, *7*(1), e1391.

Hindmarsh, A. C. (1983). Odepack, a systematized collection of ode solvers. *Scientific computing*, 55–64.

Holtgrieve, G. W., Schindler, D. E., Branch, T. A., & A'mar, Z. T. (2010). Simultaneous quantification of aquatic ecosystem metabolism and reaeration using a bayesian statistical model of oxygen dynamics. *Limnology and Oceanography*, *55*(3), 1047–1063.

Holtgrieve, G. W., Schindler, D. E., & Jankowski, K. (2016). Comment on demars et al. 2015,"stream metabolism and the open diel oxygen method: Principles, practice, and perspectives". *Limnology and Oceanography: Methods*, *14*(2), 110–113.

Hotchkiss, E., Hall Jr, R., Sponseller, R., Butman, D., Klaminder, J., Laudon, H., ... Karlsson, J. (2015). Sources of and processes controlling co2 emissions change with the size of streams and rivers. *Nature Geoscience*, *8*(9), 696–699.

Jassby, A. D., & Platt, T. (1976). Mathematical formulation of the relationship between photosynthesis and light for phytoplankton. *Limnology and oceanogra-*

phy, *21*(4), 540–547.

Koschorreck, M., Prairie, Y. T., Kim, J., & Marcé, R. (2021). Co2 is not like ch4–limits of and corrections to the headspace method to analyse pco2 in water. *Biogeosciences*, *18*, 1619–1627.

Kurz, M. J., Drummond, J. D., Martí, E., Zarnetske, J. P., Lee-Cullin, J., Klaar, M. J., ... Fleckenstein, J. H. (2017). Impacts of water level on metabolism and transient storage in vegetated lowland rivers: Insights from a mesocosm study. *Journal of Geophysical Research: Biogeosciences*, *122*(3), 628-644.

Lees, M. J., & Camacho, L. (2000). Modelling solute transport in rivers under unsteady flow conditions—an integrated velocity conceptualisation. british hydrological society. In *7th national hydrology symposium. newcastle, sept* (pp. 4–6).

Lees, M. J., Camacho, L., & Whitehead, P. (1998). Extension of the quasar river water quality model to incorporate dead-zone mixing. *Hydrology and Earth System Sciences*, *2*(2/3), 353–365.

Lees, M. J., Camacho, L. A., & Chapra, S. (2000). On the relationship of transient storage and aggregated dead zone models of longitudinal solute transport in streams. *Water Resources Research*, *36*(1), 213-224.

Manson, J., Demars, B., Wallis, S., & Mytnik, V. (2010). A combined computational and experimental approach to quantifying habitat complexity in scottish upland streams. *Proceedings of Hydropredict*.

Manson, J., Wallis, S. G., & Hope, D. (2001). A conservative semi-lagrangian transport model for rivers with transient storage zones. *Water Resources Research*, *37*(12), 3321–3329.

Martinsen, K. T., Kragh, T., & Sand-Jensen, K. (2018). A simple and cost-efficient automated floating chamber for continuous measurements of carbon dioxide gas flux on lakes. *Biogeosciences*, *15*(18), 5565–5573.

Moe, T. F., & Demars, B. O. L. (2017). *Årsrapport krypsivovervåking 2017* (Tech. Rep. No. 7202-2017). Norsk institutt for vannforskning.

Mulholland, P., Fellows, C., Tank, J., Grimm, N., Webster, J., Hamilton, S., ... Dodds, W. (2001). Inter-biome comparison of factors controlling stream metabolism. *Freshwater biology*, *46*(11), 1503-1517.

Odum, H. T. (1956). Primary production in flowing waters. *Limnology and Oceanog-*

raphy, *1*(2), 102–117.

Palumbo, J. E., & Brown, L. C. (2014). Assessing the performance of reaeration prediction equations. *Journal of Environmental Engineering*, *140*(3), 04013013.

Pathak, D. (2022, October). *MUFT model.* Zenodo. Retrieved from `https://doi.org/10.5281/zenodo.7197544` doi: 10.5281/zenodo.7197544

Pathak, D., Hutchins, M., Brown, L. E., Loewenthal, M., Scarlett, P., Armstrong, L., ... Old, G. (2022). High-resolution water-quality and ecosystem-metabolism modeling in lowland rivers. *Limnology and Oceanography*.

Payn, R. A., Hall Jr, R., Kennedy, T. A., Poole, G. C., & Marshall, L. A. (2017). A coupled metabolic-hydraulic model and calibration scheme for estimating whole-river metabolism during dynamic flow conditions. *Limnology and Oceanography: Methods*, *15*(10), 847-866.

Poff, N. L., & Zimmerman, J. K. (2010). Ecological responses to altered flow regimes: a literature review to inform the science and management of environmental flows. *Freshwater Biology*, *55*(1), 194-205.

Pulg, U., Stranzl, S., Vollset, K. W., Barlaup, B. T., Olsen, E., Skår, B., & Velle, G. (2016). *Gassmetning i otra nedenfor brokke kraftverk* (Tech. Rep. No. 1892-8889). NORCE Norwegian Research Centre AS.

Raymond, P. A., Hartmann, J., Lauerwald, R., Sobek, S., McDonald, C., Hoover, M., ... others (2013). Global carbon dioxide emissions from inland waters. *Nature*, *503*(7476), 355–359.

Raymond, P. A., Zappa, C. J., Butman, D., Bott, T. L., Potter, J., Mulholland, P., ... Newbold, D. (2012). Scaling the gas transfer velocity and hydraulic geometry in streams and small rivers. *Limnology and Oceanography: Fluids and Environments*, *2*(1), 41–53.

Rørslett, B. (1988). Aquatic weed problems in a hydroelectric river: the r. otra, norway. *Regulated Rivers: Research & Management*, *2*(1), 25–37.

Runkel, R. L. (1998). *One-dimensional transport with inflow and storage (otis): A solute transport model for streams and rivers* (Vol. 98). US Department of the Interior, US Geological Survey.

Santos Santos, T. F., & Camacho, L. A. (2022). An integrated water quality model to support multiscale decisions in a highly altered catchment. *Water*, *14*(3), 374.

Segatto, P. L., Battin, T. J., & Bertuzzo, E. (2020). Modeling the coupled dynamics of stream metabolism and microbial biomass. *Limnology and Oceanography*, *65*(7), 1573–1593.

Segatto, P. L., Battin, T. J., & Bertuzzo, E. (2021). The metabolic regimes at the scale of an entire stream network unveiled through sensor data and machine learning. *Ecosystems*, 1–18.

Sincock, A. M. (2002). *Conceptual river water quality modelling under dynamic conditions* (Unpublished doctoral dissertation). Imperial College London.

Sincock, A. M., & Lees, M. (2002). Extension of the quasar river-water quality model to unsteady flow conditions. *Water and Environment Journal*, *16*(1), 12–17.

Sincock, A. M., Wheater, H. S., & Whitehead, P. G. (2003). Calibration and sensitivity analysis of a river water quality model under unsteady flow conditions. *Journal of Hydrology*, *277*(3-4), 214–229.

Song, C., Dodds, W. K., Rüegg, J., Argerich, A., Baker, C. L., Bowden, W. B., ... others (2018). Continental-scale decrease in net primary productivity in streams due to climate warming. *Nature Geoscience*, *11*(6), 415–420.

Spear, R. C., & Hornberger, G. (1980). Eutrophication in peel inlet—ii. identification of critical uncertainties via generalized sensitivity analysis. *Water research*, *14*(1), 43–49.

Standing Committee of Analysts. (1989). *5 day biochemical oxygen demand (bod5)* (Tech. Rep.).

Streeter, H., & Phelps, E. B. (1925). *A study of the pollution and natural purification of the ohio river. iii. factors concerned in the phenomena of oxidation and reaeration* (Tech. Rep. No. 146). United States Public Health Service.

Uehlinger, U., Kawecka, B., & Robinson, C. (2003). Effects of experimental floods on periphyton and stream metabolism below a high dam in the swiss alps (river spöl). *Aquatic Sciences*, *65*(3), 199–209.

Vandenberghe, V., Van Griensven, A., & Bauwens, W. (2001). Sensitivity analysis and calibration of the parameters of eswat: Application to the river dender. *Water Science and Technology*, *43*(7), 295–301.

Venables, W., & Ripley, B. (2002). *Modern applied statistics with s fourth edition. world.*

Von Schiller, D., Acuña, V., Aristi, I., Arroita, M., Basaguren, A., Bellin, A., ... Kalogianni, E. (2017). River ecosystem processes: A synthesis of approaches, criteria of use and sensitivity to environmental stressors. *Science of the Total Environment*, *596*, 465-480.

Wagner, R. J., Boulger Jr, R. W., Oblinger, C. J., & Smith, B. A. (2006). *Guidelines and standard procedures for continuous water-quality monitors: station operation, record computation, and data reporting* (Tech. Rep.).

Wallis, S. G., & Manson, J. R. (2018). Flow dependence of the parameters of the transient storage model. In *Free surface flows and transport processes* (pp. 477–488). Springer.

Wallis, S. G., Young, P., & Beven, K. (1989). Experimental investigation of the aggregated dead zone model for longitudinal solute transport in stream channels. *Proceedings of the Institution of Civil Engineers*, *87*(1), 1-22.

Webster, J. R., Mulholland, P. J., Tank, J. L., Valett, H. M., Dodds, W. K., Peterson, B. J., ... others (2003). Factors affecting ammonium uptake in streams–an inter-biome perspective. *Freshwater Biology*, *48*(8), 1329–1352.

Weiss, R. F. (1970). The solubility of nitrogen, oxygen and argon in water and seawater. In *Deep sea research and oceanographic abstracts* (Vol. 17, pp. 721–735).

Whitehead, P., Williams, R., & Lewis, D. (1997). Quality simulation along river systems (quasar): model theory and development. *Science of the Total Environment*, *194*, 447-456.

Wright, R. F., Couture, R.-M., Christiansen, A. B., Guerrero, J.-L., Kaste, Ø., & Barlaup, B. T. (2017). Effects of multiple stresses hydropower, acid deposition and climate change on water chemistry and salmon populations in the river otra, norway. *Science of The Total Environment*, *574*, 128–138.

Yang, H., Andersen, T., Dörsch, P., Tominaga, K., Thrane, J.-E., & Hessen, D. O. (2015). Greenhouse gas metabolism in nordic boreal lakes. *Biogeochemistry*, *126*(1), 211–225.

Ye, S., Covino, T. P., Sivapalan, M., Basu, N. B., Li, H.-Y., & Wang, S.-W. (2012). Dissolved nutrient retention dynamics in river networks: A modeling investigation of transient flows and scale effects. *Water Resources Research*, *48*(6).

Young, R. G., Matthaei, C. D., & Townsend, C. R. (2008). Organic matter break-

down and ecosystem metabolism: functional indicators for assessing river ecosystem health. *Journal of the North American Benthological Society*, *27*(3), 605-625.

Zimmerman, J. K., Letcher, B. H., Nislow, K. H., Lutz, K. A., & Magilligan, F. J. (2010). Determining the effects of dams on subdaily variation in river flows at a whole-basin scale. *River Research and Applications*, *26*(10), 1246-1260.